Formation of tethered bilayer lipid membranes probed by various surface sensitive techniques

Inga K. Vockenroth
Max Planck Institute for Polymer Research, 55021 Mainz, Germany and University of Bath, Bath BA2 7AY, United Kingdom

Claire Rossi
Université de Technologie, 60200 Compiègne, France

Muhammad Raza Shah
HEJ Research Institute of Chemistry, University of Karachi, Karachi 75270 Pakistan

Ingo Köper[a)]
Max Planck Institute for Polymer Research, 55021 Mainz, Germany

(Received 30 January 2009; accepted 30 March 2009; published 30 April 2009)

Tethered bilayer lipid membranes are promising biomimetic architectures. Their formation has been investigated using four different surface sensitive techniques, including optical, acoustic, and electrical methods. The lipid bilayers are built in a two-step procedure; the proximal layer is formed by self-assembly and is then completed to a bilayer by fusion with small vesicles. The different technical approaches revealed specific aspects of the layer formation processes, namely, first a fast adsorption process followed by a longer rearrangement period. Similar phenomena have been observed for the vesicle fusion process. The results allow for a more controlled assembly protocol for the preparation of highly insulating lipid membranes. © *2009 American Vacuum Society.*
[DOI: 10.1116/1.3122019]

I. INTRODUCTION

The coating of an interface with thin films is a common way to design surface properties. An easy and versatile method is the formation of such films by self-assembly. The self-assembly process was first described in 1946 and it offers an appealing alternative to Langmuir–Blodgett films.[1] The process is a self-organization phenomenon: organic molecules adsorb spontaneously from solution to a surface and form a monomolecular layer. This process is driven by specific interactions between the organic molecules and the surface and favored by the interplay between the molecules. However, there is still lack in understanding of the detailed adsorption phenomenon.[2–7]

A self-assembled monolayer (SAM) can be defined as a functional assembly of molecules. These molecules typically have a head group that interacts with or binds to a surface. Often gold is used as support and thiol chemistry can be used to anchor the SAM to the substrate. For other surfaces such as glass or silicon, silane chemistry can be used.

The interaction between the molecules is driven by hydrophobic interactions, van der Waals attractions, or hydrogen bonding. These forces lead to the assembly of an ordered, highly reproducible, and stable layer; even after removal from the self-assembly media.[6] The functionality and the hydrophobicity of the monolayer can be adjusted by different end groups of the monolayer molecules. The stability of a SAM strongly depends on the chain length of the used alkane thiols or alkane silanes. For short chain lengths, the structures are disordered with a low packing density and low surface coverage, while hydrocarbon chains with more than ten carbon atoms assemble in a crystalline or semicrystalline state.[8,9] Chain lengths of 10–18 carbon atoms are ideal for air stable layers with high packing densities.[10,11] Such molecules form densely packed, crystallinelike layers.[8] One of the earliest works on the adsorption kinetics of long alkane thiol chains on gold surfaces reports a two-step process for the self-assembly. The first step consists in the fast adsorption of the molecules to the surface. The thickness of the adsorbed layer reaches 80%–90% of its final value within a few minutes. The second step is much slower and is dominated by the organization and rearrangements of the monolayer. Displacement of contaminants and expulsion of included solvent may also be involved in this slow step,[12] which can take several hours up to days.[6,13,14] Several reports have confirmed the two-step adsorption process by using different methods such as ellipsometry and contact angle (wettability) measurements,[12] x-ray photoelectron spectroscopy,[15] IR-visible sum frequency spectroscopy,[13,14] surface plasmon resonance (SPR) spectroscopy,[16] atomic force microscopy (AFM),[17] or quartz crystal microbalance (QCM).[18]

SAMs can be used as functional coatings of substrates. A possible application is to use the film as supporting layer for solid supported membranes. On top of a hydrophobic SAM, a second lipid monolayer can be deposited by either vesicle fusion,[19] solvent exchange,[20] or horizontal Langmuir film transfer.[21] Depending on the nature of the surface and the external parameters such as temperature, *p*H, and ionic strength, vesicles interact with the surface in different ways.[22–24] Fusion of vesicles on hydrophilic supports is well described and involves adsorption, rupture, and spreading.[25]

[a)]Electronic address: ingo.koeper@mpip-mainz.mpg.de

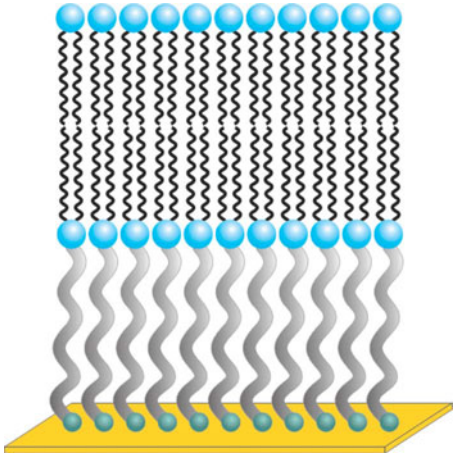

FIG. 1. (Color online) Schematic depiction of the tethered membrane architecture. The inner leaflet is covalently bound to a substrate via a spacer unit; the distal layer is formed by vesicle fusion.

There have been several studies investigating the unrolling of vesicles on hydrophobic surfaces; however, the precise mechanism involved in the fusion process is not known. Lingler *et al.* proposed a mechanism that involves approach, adhesion, rupture, and lateral spreading of the monolayer.[11]

In case of tethered bilayer lipid membranes (tBLMs), the proximal layer consists of a lipid layer, which is covalently attached to a solid support by a spacer group (Fig. 1). Membranes based on the anchorlipid 2,3-di-O-phytanyl-glycerol-1-tetraethylene glycol-D,L-lipoic acid ester lipid (DPhyTL) have been shown to form dense layers with high electrical sealing properties.[26–31]

In order to study the detailed assembly processes of the system, a combination of different techniques has been used. The high spatial resolution of the AFM was used to probe topographic changes during the assembly processes. SPR spectroscopy and quartz crystal microbalance with dissipation (QCM-D) gave insights into the assembly kinetics with a high time resolution. Finally, the electrochemical sealing properties of the mono- and bilayer were investigated using electrochemical impedance spectroscopy (EIS). Recently, a similar study has been published; however, we find quite different results. Dorvel *et al.* reported on the fusion of anchorlipid vesicles in the formation of the monolayer, which is not very probable, since the lipids are completely soluble in ethanol.[32] Furthermore, the combination of electrical and optical techniques offers more insight into the processes.

II. MATERIALS AND METHODS

The synthesis of DPhyTL was performed as previously described.[29] Diphytanoylphosphatidylcholine (DPhyPC) was from Avanti Polar Lipids Inc. (Alabaster, AL). Ethanol (chromatography grade) and sodium chloride (SigmaUltra) were purchased from Sigma-Aldrich. All measurements and assembly processes were performed at room temperature.

A. Template stripped gold preparation

Template stripped gold (TSG) was prepared according to a procedure described previously.[28,33] 48 nm of gold are evaporated onto a clean silicon wafer (CrysTec, Berlin, Germany), glued with an epoxy glue (Epo-Tek 353ND4, Polytec, Waldbronn, Germany) to a glass slide, and cured at 150 °C for 1 h. Stripping of the silicon wafer reveals an extremely flat gold surface that is used immediately for the experiments.[26] If not stripped, the samples can be stored for weeks before use.

B. Formation of the DPhyTL self-assembled monolayer and vesicle fusion

The proximal layer was assembled from ethanolic solutions of DPhyTL at various concentrations onto TSG slides. For QCM-D, SPR, and EIS measurements, a concentration of 0.2 mg/ml was used. For AFM measurement, a reduced DPhyTL concentration of 5 μg/ml was used in order to slow down the assembly process. When the formation process was not monitored *in situ*, TSG slides were taken out of the DPhyTL solution, rinsed with pure ethanol, and dried in a stream of nitrogen just before being inserted in the measurement cell. The possible existence of DPhyTL vesicles in a solution at 5 μg/ml in ethanol was investigated by quasi-elastic light scattering (Zetasizer 1000/3000, Malvern Instruments, UK).

Unilamellar DPhyPC vesicles were prepared from concentrated DPhyPC solution in MilliQ water by extrusion through 50 nm polycarbonate filters (Aventi). The distal layer was assembled onto DPhyTL monolayers after 24 h self-assembly by addition of small unilamellar vesicles (final concentration of 0.02 mg/ml in a NaCl solution of 0.1 mol/l).

C. Atomic force microscopy

AFM measurements were performed in liquid using a Nanoscope IIIa (Multimode, Veeco Instruments, CA) at a scan rate of 0.5–1 Hz and a pixel number of 512×512. AFM images were acquired in tapping mode at room temperature in a liquid cell and repeated several times with different samples to ensure reproducibility. AFM disks are used instead of the glass substrate to enable the use of a commercial, tightly sealing flow cell. Silicon nitride cantilevers (Nanoworld, Switzerland; 240 μm long, 30 μm wide, 2.8 μm thick) with a nominal spring constant of 0.7–3.8 N/m, an integrated tip (radius <10 nm), and a resonance frequency of 70 kHz were plasma cleaned prior to use. The tip was typically scanned at a velocity from 0.5 to 1 μm s^{-1}. Height and phase images were used to analyze the topographic changes. Images were flattened and the roughness and line scans analyzed as indicated.

D. Electrochemical impedance spectroscopy

EIS measurements were conducted using an Autolab spectrometer (Eco Chemie, Utrecht, The Netherlands). Spectra were recorded for frequencies between 2 MHz and 100 kHz at 0 V bias potential with an ac modulation amplitude of

10 mV. Raw data were analyzed using the ZVIEW software package (Version 2.90, Scribner Associates). Three-electrode measurements were performed with the substrate as the working electrode, a coiled platinum wire as the counter electrode, and a DRIREF-2 reference electrode (World Precision Instruments, Berlin, Germany).

The experimental data have been analyzed using a model equivalent circuit of resistors (R) and capacitors (C).[34] The different components can be attributed to the individual parts of the membrane architecture. An $R(RC)C$ circuit consisting of an RC element describing the mono- or bilayer in series with a capacitor (C_{SC}) and an electrolyte resistance ($R_{electrolyte}$) [see inset in Fig. 5(a)] has been used. C_{SC} represents the space charge capacitance due to the spacer region combined with the capacitive effects of the electrochemical double layer at the gold interface.[28,35] In the case of low monolayer resistances, an additional resistance attributed to the spacer region can be seen; therefore, an $R(RC)(RC)$ circuit has been used.[36]

EIS data can be visualized in Bode plots (see Fig. 7), where pure capacitances show up as slopes of -1 with high phase shifts of $-90°$ and ideal resistances are represented as horizontal regions of low phase angles.[34] An alternative representation is the admittance plot (see inset in Fig. 4), where the frequency reduced real part of the admittance ($Y=1/Z$) is plotted versus the imaginary part. RC elements can be identified as semicircles. The intersection on the y axis corresponds to the capacitance, while resistances give a line parallel to the y axis.

E. SPR spectroscopy

A customized instrument in the Kretschmann configuration with a He/Ne laser ($\lambda=632$ nm) was used. In the kinetic mode, changes in reflectivity at a fixed angle are monitored as a function of time. The angular SPR spectra (not shown) were analyzed using a three layer model including the prism, gold, and thiolipid monolayer. After vesicle fusion a fourth layer corresponding to the outer leaflet of the bilayer was added to the model. The refractive indices of $n=1.5$ and $n=1.45$ for the mono- and bilayer, respectively, were used.[26]

F. QCM-D

Measurements were performed with the Q-Sense E4 instrument (Q-Sense, Gothenburg, Sweden). To avoid hydrocarbon contamination, the bare gold sensors were treated first with an argon plasma (300W, 5 min) and then immersed in a freshly prepared solution of 5:1:1 H_2O/H_2O_2 (35%)/NH_3 (30%) at 70 °C for 5 min. The sensors were intensely rinsed with ultrapure water and ethanol and dried in a nitrogen stream and mounted in the sensor chambers. For sample injection and rinsing steps, solutions (400 μl) were pumped through the sensor chamber by a peristaltic pump at a flow rate of 200 μl/min.

Changes in frequency, related to attached mass (including coupled water), and dissipation, related to frictional (viscous) loss in the layer, were recorded as a function of time. Resonance frequency and dissipation were simultaneously measured at several harmonics ($n=15,25,35$ MHz). In the case of dense and rigid layers, the normalized frequency change ($\Delta f_n/n$) is represented as the acoustic thickness (d) increase according to the Sauerbrey equation[37]

$$d=\frac{\Delta m}{\rho}=\frac{-C\times\Delta f_n}{n\times\rho},$$

with $C=17.7$ ng Hz cm^{-2} and ρ the effective density of the dielectric layer, assumed to be 1.2 g ml^{-1}. This equation has been validated for lipid bilayers on surfaces.[23,38]

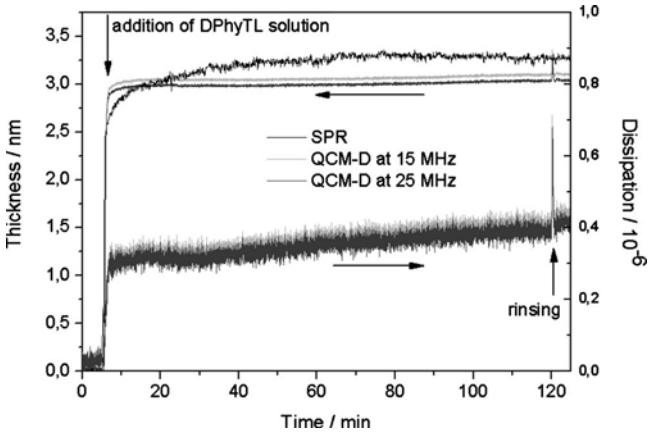

FIG. 2. Adsorption kinetic of DPhyTL from 0.2 mg/ml ethanol solution followed by QCM-D and SPR. Frequency shift response (Sauerbrey thickness) at 15 and 25 MHz and optical thickness and changes in dissipation at 15 and 25 MHz as a function of time. Arrows indicate the addition of the monolayer solution and the rinse with ethanol.

III. RESULTS AND DISCUSSION

The membrane architecture consists two layers, i.e., a SAM formed of anchorlipids and a distal lipid layer formed by vesicle fusion (Fig. 1). First, the assembly process of the monolayer was analyzed by monitoring changes in thickness, topography, and electrochemical properties of the film. The anchorlipids (DPhyTL) consist of two hydrophobic chains that are coupled to a short oligometic spacer, which is functionalized with a lipoic acid moiety.

1. Monolayer assembly

For SPR and QCM-D experiments, substrates were mounted into the respective flow cells and measured in ethanol. After 5 min, the DPhyTL solution (0.2 mg/ml) was injected and the changes in frequency, dissipation, and reflectivity were monitored as a function of time (Fig. 2). The kinetics of the monolayer formation was very fast and saturated after 10 min for QCM-D and after about 1 h for SPR. The difference in the time scale could be explained by difference in the injection mode. For SPR experiments, the cell was emptied and refilled with the DPTL solution. For QCM-D measurements, the DPTL solution was injected into the filled cell by using a peristaltic pump. Thus, a higher

volume (400 μl) of DPTL solution is used. In fact, the surface is exposed to four times higher quantity of DPTL than in the SPR experiment.

The total frequency shift was $\Delta f = -17$ Hz. The energy dissipation, which gives information about the viscoelastic properties of the adsorbed film, stabilized around $\Delta D = 0.4 \times 10^{-6}$, indicating the presence of a rigid DPhyTL film at the surface. The total frequency changes in QCM-D could be analyzed using the Sauerbrey equation. The Sauerbrey mass density was 300 ng/cm^2 and the obtained acoustic thickness of 3.0 ± 0.3 nm was in good agreement with the optical thickness of 3.1 ± 0.3 nm monitored by SPR (from three independent measurements).

The results obtained in this study are quite different to those published by Dorvel *et al.*[32] They showed a biphasic kinetic curve for the adsorption and reorganization of the DPhyTL into a self-assembled monolayer. The QCM monitoring of DPhyTL deposition at 300 μM ($\sim 1 \times 10^{-4}$ mg/ml) on gold showed a linear frequency shift, which reached -15 Hz after 5 h, followed by a stronger frequency decrease from 8 to 21 h until a plateau at a frequency shift of $\Delta f \sim -50$ Hz was reached. In the same way, the dissipation reached 1.5 and 13 after 5 and 24 h of incubation time, respectively. The authors proposed the swelling of the monolayer in ethanol as an explanation of the second phase in frequency and dissipation changes. Our results are in accordance with the frequency and dissipation values obtained after 5 h. However, a second phase was never observed. After the plateau phase, dissipation and the frequency remained constant for 24 h (data not shown). The duration of the first phase depended on the DPhyTL concentration (see supporting information); however, the final layer thicknesses in terms of frequency shift or optical thickness were identical.

However, an increase in thickness of a DPhyTL SAM has been observed in NaCl solution by using SPR spectroscopy.[28] This could be confirmed by using QCM-D techniques (see supporting information). A slow frequency decrease and a dissipation increase were observed after exchange of ethanol by 0.1*M* NaCl solution. The stabilization occurs after 7 h with a frequency and dissipation shift of $\Delta f = -6$ Hz and $\Delta D = 1.8 \times 10^{-6}$, respectively. A Sauerbrey conversion of frequency shift led to a thickness increase of 1 nm, corresponding to the value reported previously.[28] These changes in frequency and dissipation could be explained by the relaxation of the poly(ethylene)glycol (PEG) chains in the electrolyte solution; the frequency shift could be attributed to the increase in the mass of water coupled into the SAM and the variation of dissipation to the relative increase in the flexibility of the PEG chains.

AFM was used to monitor the change in the local organization of the layer during the self-assembly process. A freshly stripped gold substrate was mounted into a liquid cell, ethanol was injected, and the bare gold surface was monitored [Fig. 3(a)], followed by addition of the thiolipid solution. In order to be able to resolve the different assembly steps by AFM, the assembly process has been slowed down. This has been achieved by reducing the DPhyTL concentration with respect to the other techniques to 5 μg/ml. Subsequent scans were taken at various time intervals [Figs. 3(b)–3(f). From the obtained images and the cross-sectional analyses the most important features during the self-assembly process could be investigated.

The anchorlipids adsorbed first at the surface, which resulted in small island formation [Figs. 3(b) and 3(c)]. As indicated from the low peak to valley distances, the molecules were mostly lying flat on the surface. The packing density increased with time and the thickness increased even above the final monolayer thickness [see linescan in Fig. 3(d)] and the roughness decreased. Probably, surface aggregates of stacked molecules were formed. Dorvel *et al.* interpreted such structures as adsorbed vesicles;[32] however, the size dimensions do not match this assumption. As a confirmation, by quasielastic light scattering measurements, no DPhyTL vesicles could be detected in ethanolic solution. The surface structures were not stable when a higher coverage was reached at longer assembly times. After 12 h [Fig. 3(e)], singular islands and patches of 3 nm height could be imaged, where the anchorlipids reached their final upright conformation. During the next hours the islands grew until a uniform film was formed after 24 h [Fig. 3(f)]. The final monolayer had a roughness of 0.27 nm and a thickness of 3 nm. Hardly any defects were visible.

For EIS measurements, monolayers on TSG with increasing assembly times between 1 min and 24 h (Fig. 4) were prepared. The observation of *in situ* kinetics is not possible, since impedance measurements are not practicable in ethanol. The same assembly solution was used for all slides, as the amount of actually adsorbed material is negligible with respect to the total concentration. Five impedance spectra were recorded for every sample starting with a freshly stripped TSG slide. With increasing assembly times, the impedance shifted to higher resistances and lower capacitances (Table I).

Data could be analyzed using an $R(RC)(RC)$ circuit for all but the two last assembly times, for which the standard $R(RC)C$ circuit was used,[27,29] as the space charge resistance disappeared with higher monolayer resistances. The bare gold slide showed a capacitance of about 47 μF cm^{-2}, in agreement with literature values for a pure gold capacitance (10–50 μF cm^{-2}).[39,40] The space charge capacitance C_{SC} decreased with time, corresponding to an increase in spacer thickness during the monolayer formation. For the disordered layers at the beginning of the assembly process, a thin spacer region can be assumed, which increases in thickness as the film grows. Due to the same effects, the space charge resistance increases until it is too high to be determined in the observed frequency range.

All electrical parameters showed, similar as SPR and QCM, a rapid first phase of the assembly (Table I). As seen by AFM, the molecules rapidly cover the surface; however, the formation of a densely packed and defect-free layer takes longer. Repulsive forces between adsorbed and free molecules probably hinder the completion of defects in the layer.

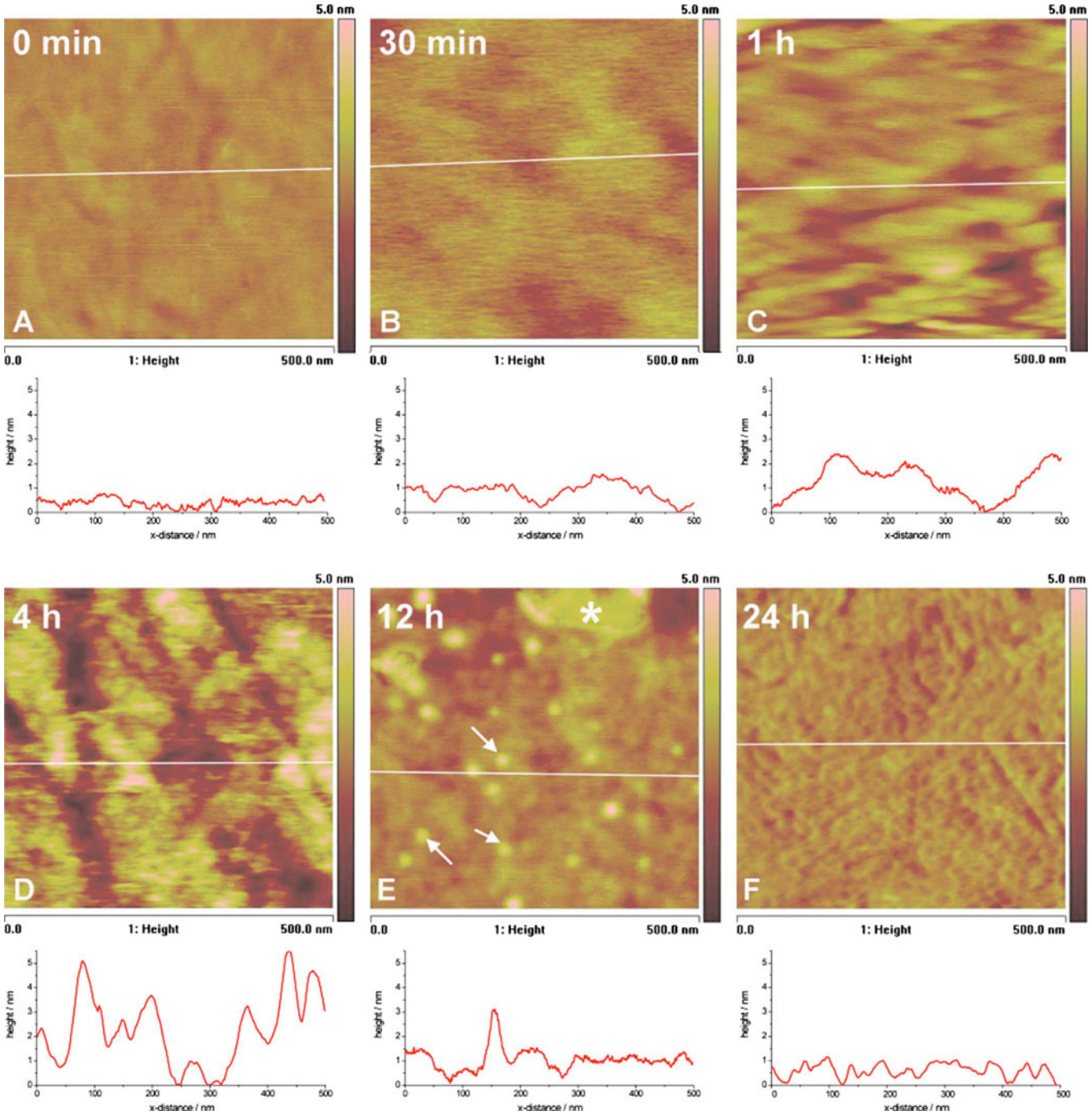

FIG. 3. (Color online) Selected AFM height images recorded at different assembly times, showing the formation of a self-assembled monolayer. The linescans below the images show the initial increase in roughness due to the formation of aggregates and the final roughness of the monolayer. The arrows in image (e) indicate small islands of monolayer molecules; the asterisk shows a large monolayer patch with 3 nm height.

After 24 h, the highest coverage is reached and the electrical properties do not improve further. In summary, the formation of a lipid monolayer is a two-step process, similar to the known adsorption processes of long alkane thiols. SPR and QCM-D techniques can only resolve the first, fast adsorption step, where already a high surface coverage is reached. In the second, slow assembly step, rearrangements in the layer take place, as seen by AFM and EIS. Both techniques showed a complete monolayer formation after about 24 h. SPR and QCM-D are not sensitive enough to detect such changes.

2. Bilayer assembly

Monolayers after 24 h of assembly time have been used and then completed to bilayer by fusion of vesicles. The process has been investigated by the four different techniques.

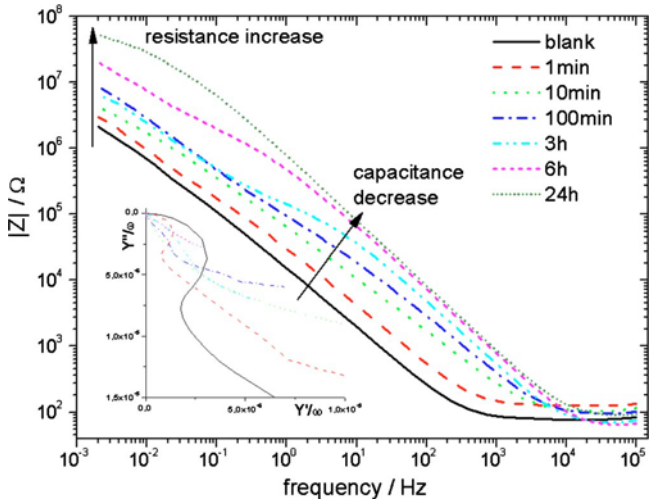

FIG. 4. (Color online) TSG slides were left for varying assembly times in DPhyTL and then investigated for their electrochemical properties by impedance spectroscopy. The impedance scans show the increase in resistance with longer assembly times. The inset shows the corresponding admittance plot where the capacitance decrease with longer assembly times can be seen by a decrease of the semicircle.

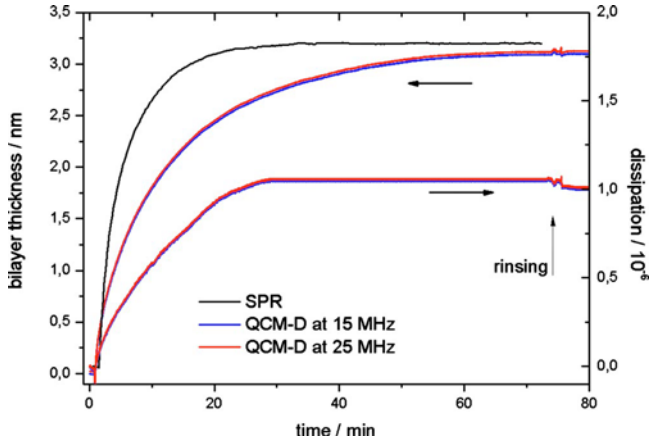

FIG. 5. (Color online) QCM-D and SPR response for the fusion of DPhyPC vesicles with a DPhyTL monolayer. Frequency shift response (Sauerbrey thickness) at 15 and 25 MHz and optical thickness as a function of time and changes in dissipation at 15 and 25 MHz. The arrow indicates rinse with buffer.

In order to eliminate additional changes in reflectivity, frequency, and dissipation, induced by the DPhyTL monolayer swelling, the DPhyPC vesicles were injected into the measurement cells after stabilization of swelling process. Similar to the monolayer formation, SPR and QCM-D experiments showed a fast kinetics with an exponential increase in thickness that equilibrated in less than 1 h (Fig. 5). The shift in frequency reached -17.5 Hz and the calculated thickness of the distal layer was 3.1 ± 0.3 nm (for three independent measurements) for both SPR and QCM-D, indicating a dense layer that contains little water. Only a small increase in dissipation was observed after addition of the vesicles. On the DPhyTL monolayer, no adsorption was observed and the fusion rather was a continuous process. After rinsing, the bilayer was stable and the dissipation reached a value of 1.0×10^{-6}.

The shift in frequency was between values obtained for vesicle fusion of an egg phosphatidylcoline (EggPC) layer on the top of an alkane thiol monolayer (-13 Hz) and values obtained after bilayer formation on a hydrophilic surface (-26 Hz).[38] The values obtained for the acoustic and optical thicknesses are in accordance with the structure of the DPhyPC molecules. Moreover, the QCM-D curves are similar to those obtained for vesicle fusion on hydrophobic layers of dense alkyl SAMs.[38] The characteristic transition phase, observed for the fusion of vesicles on hydrophilic surfaces, was not observed. This phase was described as corresponding to the distinctive initial adsorption of intact vesicles and their disruption to form the lipid layer.[23,38] In case of vesicle fusion on hydrophobic surfaces as on top of a DPhyTL monolayer, the process seems to be a rather direct fusion. The process is probably mostly driven by hydrophobic interactions between the SAM and the lipids of the vesicles.

TABLE I. Resistance and capacitance values for the different assembly times of a DPhyTL monolayer showing the development of a highly sealing membrane after 24 h.

Assembly time	$R_{monolayer}$ (kΩ cm^2)	$C_{monolayer}$ (μF cm^{-2})	C_{SC} (μF cm^{-2})	R_{SC} (MΩ cm^2)
Blank	7.73	47.21	68.26	0.54
1 min	14.08	18.02	44.58	0.77
10 min	16.32	4.40	18.91	0.99
100 min	22.6	2.32	14.25	2.29
3 h	41.6	1.33	15.7	1.63
6 h	624	0.96	9.66	
24 h	9.4×10^3	0.77	10.77	

The final dissipation value of 1.0×10^{-6} was higher than values observed for silica supported lipid bilayers (0.2×10^{-6}).[23,38] This could be due to the initial swelling of the PEG chains of the DPhyTL molecules that increases the flexibility of the final structure (see supporting information).[41]

For AFM measurements, vesicles were added to the monolayer immersed in buffer and images were recorded at different time intervals (Fig. 6). After about 10 min, disklike structures could be observed on the surface with diameters between 50 and 250 nm and a height of 5 nm [Fig. 6(a)]. Probably, these were adsorbed and hemifused vesicles. Subsequently, the surface coverage increased and the vesicles seemed to roll up, as indicated by the concave geometry with a depressed center surrounded by a slightly higher rim [Fig. 6(b)]. However, artifacts due to interaction with the AFM tip cannot be fully excluded.[42] The depressed center might as well be caused by the tip pushing on a soft lipid island. A detailed picture about the complete fusion process is still unclear. After 3 h, continuous areas of bilayer patches were monitored [Fig. 6(c)]. The height of about 2 nm corresponded most probably to a tilted arrangement of the lipid

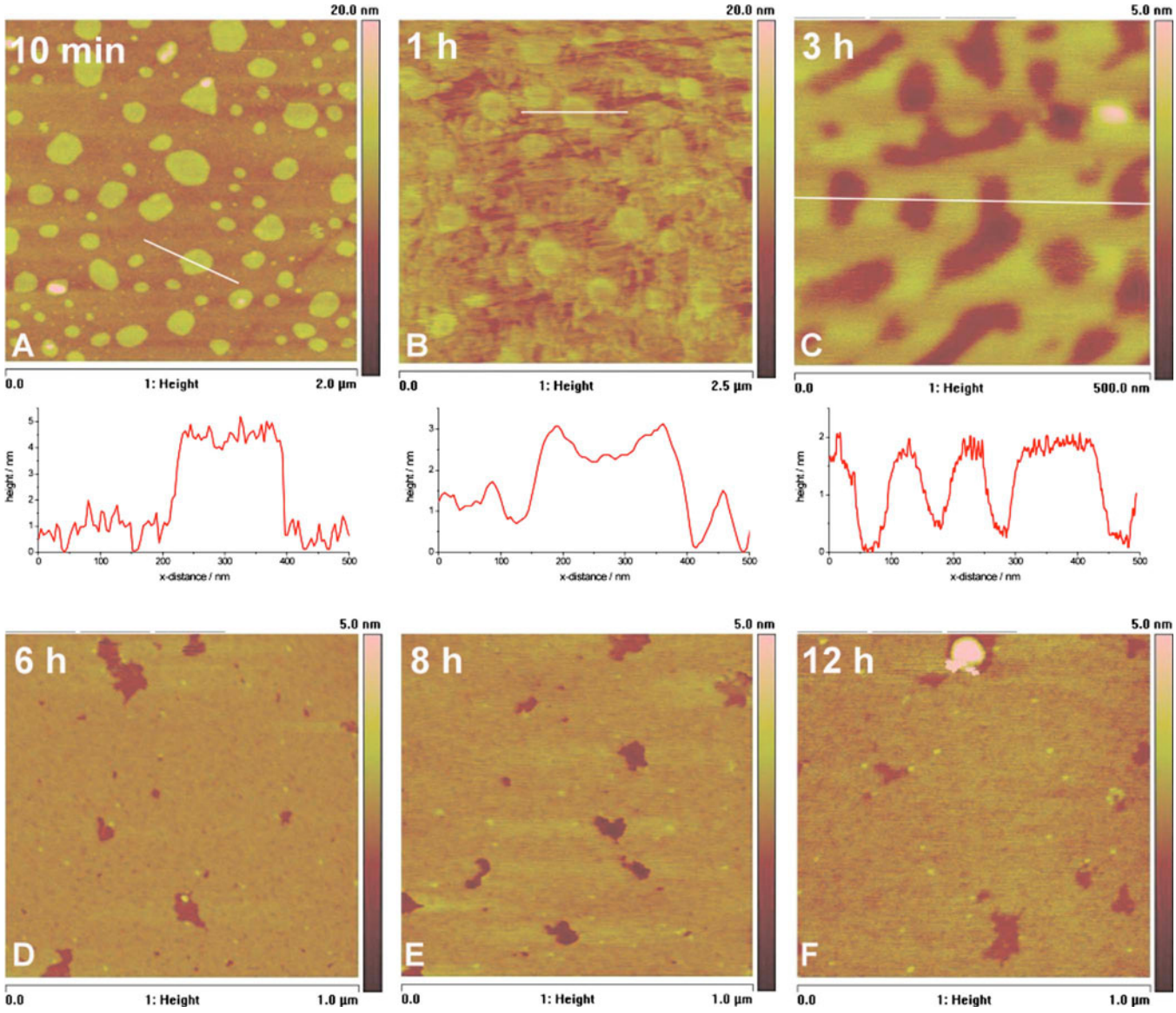

FIG. 6. (Color online) AFM height images recorded throughout the fusion of vesicles with a preformed monolayer. At the beginning vesicles adsorb and spread on the surface forming islands and after 12 h a complete layer is formed.

molecules due to the low coverage. In the following, the defects in the bilayer were filled, either by addition of new lipids or by rearrangements within the bilayer patches. After 12 h the layer was almost closed and, from the few defects, a thickness of 3 nm for the distal layer was determined [Fig. 6(f)].

Time dependent EIS measurements showed a similar trend as the AFM experiments (Fig. 7). The bilayer resistance increased first rapidly and saturated after about 7 h. The capacitance showed a similar trend.

Similar to the monolayer assembly, the different techniques probed different details of the vesicle fusion process. SPR and QCM showed a fast increase in mass at the surface, while AFM and EIS revealed further rearrangements and filling of defects occurring on a longer time scale until a homogeneous and electrically sealing bilayer was formed.

IV. CONCLUSION

Tethered bilayer membranes are versatile solid supported model membranes. Typically, they assemble in a two-step procedure. The formation of a hydrophobic monolayer by chemisorption of anchorlipids onto a solid support is followed by a fusion of the layer with vesicles. The processes involved in the formation of this architecture are similar to processes known for the formation of self-assembled monolayers and have been studied in detail using a combination of optical, acoustical, and electrical techniques. The different techniques, SPR, QCM-D, AFM, and EIS, revealed different aspects both of the monolayer formation as well as of the vesicle fusion process. In order to understand the full process of both SAM formation as well as vesicle fusion, results from all different techniques have to be discussed together.

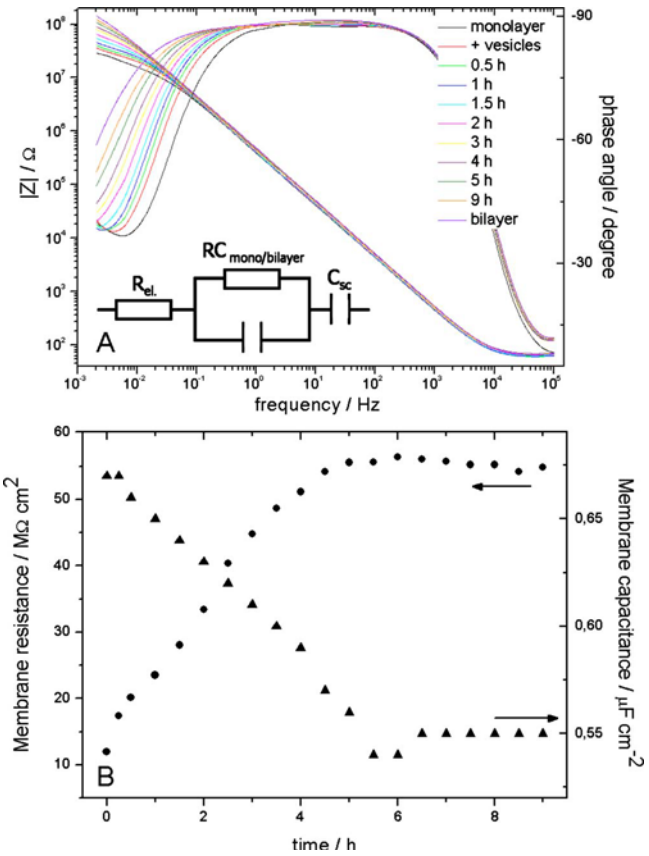

FIG. 7. (Color online) Vesicle fusion monitored by EIS on a DPhyTL-based tBLM. (a) The spectra in the Bode plot show an increase in resistance after vesicle addition. (b) The fitted resistance and capacitance values are depicted as a function of time. An increase in resistance and a capacitance drop can be seen.

For example, optically, a bilayer seemed to be formed after about 1; however, at this point, the electrical properties have not reached their ideal values. In order to control the successful bilayer formation, information over the whole time scale is needed. In order to characterize a complete bilayer, EIS seems to give the most complete picture.

The investigated processes were observed at room temperature only. It is well known that the temperature can have a significant effect on both the formation of a SAM as well as on the vesicle fusion process. It would be interesting to compare the present study with experiments at different temperatures. Additionally, the lipid composition of the vesicles also should have an effect on the assembly kinetics. Here, pure DPhyPC vesicles were used, since these lipids are often used, when electrically insulating membranes are needed. In other approaches, different lipids might be needed, which could lead to different membrane formation kinetics. However, for the presented systems, it is possible to reproducibly create high quality membranes within the determined set of parameters.

[1]W. C. Bigelow, D. L. Pickett, and W. A. Zismann, J. Colloid Sci. **1**, 513 (1946).
[2]K. L. Prime and G. M. Whitesides, Science **252**, 1164 (1991).
[3]J. S. Lindsey, New J. Chem. **15**, 153 (1991).
[4]A. Pfeil and J. M. Lehn, J. Chem. Soc., Chem. Commun. **11**, 838 (1992).
[5]J. T. Groves, N. Ulman, and S. G. Boxer, Science **275**, 651 (1997).
[6]J. Lippincott-Schwartz and W. Liu, Nature (London) **426**, 507 (2003).
[7]F. Schreiber, Prog. Surf. Sci. **65**, 151 (2000).
[8]M. D. Porter, T. B. Bright, K. K.Allara, and C. E. D. Chidsey, J. Am. Chem. Soc. **109**, 3559 (1987).
[9]S. D. Evans, R. Sharma, and A. Ulman, Langmuir **7**, 156 (1991).
[10]A. L. Plant, Langmuir **9**, 2764 (1993).
[11]S. Lingler, I. Rubinstein, W. Knoll, and A. Offenhýýusser, Langmuir **13**, 7085 (1997).
[12]C. D. Bain and G. M. Whitesides, J. Am. Chem. Soc. **111**, 321 (1989).
[13]M. Himmelhaus, F. Eisert, M. Biuck, and M. Grunze, J. Phys. Chem. B **104**, 576 (2000).
[14]Ch. Humbert *et al.*, Physica Status Solidi **175**, 129 (1999).
[15]C. D. Bain and G. M. Whitesides, J. Am. Chem. Soc. **111**, 7164 (1989).
[16]F. S. Damos, R. C. S. Luz, and L. T. Kubota, Langmuir **21**, 602 (2005).
[17]K. Hu and A. J. Bard, Langmuir **14**, 4790 (1998).
[18]C. Mokrani, J. Fatisson, L. Guýýrente, and P. Labbýý, Langmuir **21**, 4400 (2005).
[19]E. Kalb, S. Frey, and L. K. Tamm, Biochim. Biophys. Acta **1103**, 307 (1992).
[20]C. Miller, P. Cuendet, and M. Grätzel, J. Electroanal. Chem. Interfacial Electrochem. **278**, 175 (1990).
[21]H. M. McConnell, T. H. Watts, R. M. Weis, and A. A. Brian, Biochim. Biophys. Acta **864**, 95 (1986).
[22]H.-J. Butt and A.-K. Awizio, *Atomic Force Microscopy of Lipid Bilayers. Advances in Planar Lipid Bilayers and Liposomes* (Elsevier, New York, 2006), Vol. 3.
[23]R. Richter, A. Mukhopadhyay, and A. Brisson, Biophys. J. **85**, 3035 (2003).
[24]R. P. Richter and A. Brisson, Langmuir **19**, 1632 (2003).
[25]A. T. A. Jenkins, N. Boden, R. J. Bushby, S. D. Evans, P. F. Knowles, R. E. Miles, S. D.Ogier, H. Schýýnherr, and G. J. Vancso, J. Am. Chem. Soc. **121**, 5274 (1999).
[26]S. M. Schiller, R. Naumann, K. Lovejoy, H. Kunz, and W. Knoll, Angew. Chem. **42**, 208 (2003).
[27]I. K. Vockenroth, P. P. Atanasova, A. T. A. Jenkins, and I. Kýýper, Langmuir **24**, 496 (2008).
[28]R. Naumann *et al.*, Langmuir **19**, 5435 (2003).
[29]I. K. Vockenroth, P. P. Atanasova, J. R. Long, A. T. A. Jenkins, W. Knoll, and I. Kýýper, Biomembranes **1768**, 1114 (2007).
[30]I. Köper, Mol. Biosyst. **3**, 651 (2007).
[31]I. K. Vockenroth, C. Ohm, J. W. F. Robertson, D. J. McGillivray, M. Lýýsche, and I. Kýýper, BioInterphases **3**, FA68 (2008).
[32]B. R. Dorvel, H. M. Keizer, D. Fine, J. Vuorinen, A. Dodabalapur, and R. S. Duran, Langmuir **23**, 7344 (2007).
[33]H.-J. Butt, T. Müller, and H. Gross, J. Struct. Biol. **110**, 127 (1993).
[34]E. Barsoukov and J. R. Macdonald, *Impedance Spectroscopy—Theory, Experiment, and Applications. 2* (Wiley, Hoboken, NJ, 2005).
[35]V. Atanasov, P. P. Atanasova, I. K. Vockenroth, N. Knorr, and I. Kýýper, Bioconjugate Chem. **17**, 631 (2006).
[36]I. K. Vockenroth, D. Fine, A. Dodobalapur, A. T, A. Jenkins, and I. Kýýper, Electrochem. Commun. **10**, 323 (2008).
[37]G. Sauerbrey, Z. Phys. **155**, 206 (1959).
[38]C. A. Keller and B. Kasemo, Biophys. J. **75**, 1397 (1998).
[39]D.R. Lide, *CRC Handbook of Chemistry and Physics*, 85th ed. (CRC, Boca Raton, FL, 2004).
[40]M. B. Cortie, A. I. Maaroof, and G. B. Smith, Gold Bull. **38**, 14 (2005).
[41]See EPAPS Document No. E-BJIOBN-4-007902 for the effects of DPhyTL concentration on the assembly processes and for the swelling of DphyTL SAMs in electrolyte solution. For more information on EPAPS, see http://www.aip.org/pubserves/epaps.html.
[42]X. Liang, G. Mao, and K. Y. S. Ng, Colloids Surf., B **34**, 41 (2004).